Supporting Information for
"^{35}Cl Solid-State NMR of HCl Salts of Active Pharmaceuticals Ingredients: Structural Prediction, Spectral Fingerprinting and Polymorph Recognition"

Marcel Hildebrand,[†] Hiyam Hamaed,[†] Andrew M. Namespetra,[†] John M. Donohue,[†] Riqiang Fu,[‡] Ivan Hung,[‡] Zhehong Gan,[‡] and Robert W. Schurko[†,*]

†*University of Windsor, Department of Chemistry and Biochemistry. Windsor, Ontario, Canada N9B 3P4*

‡*National High Magnetic Field Laboratory, 1800 E. Paul Dirac Drive, Tallahassee, FL 32310 – 3706*

*Author to whom correspondence should be addressed. E-mail: rschurko@uwindsor.ca Tel: (519) 253-3000 x3548. Fax: (519) 973-7098

Table of Contents:

Additional experimental details

Sample Preparation of MexiI. 96 mg of commercial mexiletine HCl (Mexi) was dissolved 1 mL of methanol and allowed to slowly evaporate over approximately 4 days.

Sample Preparation of MexiII. Approximately 1 g of commercial mexiletine HCl (Mexi) was heated for two hours at 160 °C.

Sample Preparation of IsoxI. 547 mg of commercial isoxsuprine HCl (Isox) was placed in a Schlenk flask and dissolved in 20 ml of methanol. The solution was cooled to 0 °C then placed in an oil bath at 140 °C and the solvent rapidly removed under reduced pressure.

The generation of all polymorphs was confirmed via pXRD.

Table S1. Acquisition parameters for static ^{35}Cl SSNMR spectra (9.4 T) of Adip, Bufl, Dicy, Trig, Rani, Dibu, Scop.

	Adip	Bufl	Dicy	Trig	Rani	Dibu	Scop
Pulse sequence	Echo	Echo	Echo	Echo	Echo	Echo	Echo
Number of sub-spectra acquired	5	4	7	5	1	1	3
Transmitter offset per piece (kHz)	55	50	50	55	---	---	35
Number of scans per sub-spectrum	10320	11408	31760	9424	95064	139120	29681
Recycle delay (s)	0.5	0.5	0.5	0.5	0.5	0.5	0.5
Dwell (μs)	2.0	2.0	2.0	2.0	1.25	2.5	2.0
Spectral width (kHz)	500	500	500	500	800	400	500
Acquisition length (number of points)	512	512	512	512	512	1024	512
CT selective 90° pulse width [π/2] (μs)	1.75	1.75	1.75	1.75	1.75	1.50	1.75
CT selective 180° pulse width [π] (μs)	3.50	3.50	3.50	3.50	3.50	3.00	3.50

Table S2. Acquisition parameters for static ^{35}Cl SSNMR spectra (9.4 T) of Mexi, Brom, Alpr, Isop, Aceb, Aman, Proc.

	Mexi	Brom	Alpr	Isop	Aceb	Aman	Proc
Pulse sequence	Echo	Echo	Echo	Echo	Echo	Echo	Echo
Number of sub-spectra acquired	1	5	5	5	5	1	5
Transmitter offset per piece (kHz)	---	50	50	50	35	---	40
Number of scans per sub-spectrum	63424	30704	28992	30704	23872	20000	30464
Recycle delay (s)	0.5	0.5	0.5	0.5	0.5	0.5	0.5
Dwell (μs)	1.25	2.0	2.0	2.0	2.0	4.0	2.0
Spectral width (kHz)	800	500	500	500	500	250	500
Acquisition length (number of points)	512	512	512	512	512	512	512
CT selective 90° pulse width [π/2] (μs)	2.25	1.75	1.75	1.75	2.00	1.50	1.75
CT selective 180° pulse width [π] (μs)	4.5	3.5	3.5	3.5	4.00	3.00	3.5

Table S3. Acquisition parameters for static ^{35}Cl SSNMR spectra (9.4 T) of Isox, Dopa, Amin, IsoxI, MexiI, MexiII.

	Isox	Dopa	Amin	IsoxI	MexiI	MexiII
Pulse sequence	Echo	Echo	Echo	Echo	Echo	Echo
Number of sub-spectra acquired	4	5	1	5	1	1
Transmitter offset per piece (kHz)	50	55	---	50	---	---
Number of scans per sub-spectrum	28880	30112	153759	58000	28500	38608
Recycle delay (s)	0.5	0.5	0.5	0.5	0.5	0.5
Dwell (μs)	2.0	2.0	10.0	2.0	10.0	2.0
Spectral width (kHz)	500	500	100	500	100	500
Acquisition length (number of points)	512	512	512	512	512	512
CT selective 90° pulse width [π/2] (μs)	1.75	1.75	6.6	1.75	7.00	1.75
CT selective 180° pulse width [π] (μs)	3.50	3.5	13.2	3.50	7.00	3.50

Table S4. Acquisition parameters for static ^{35}Cl SSNMR spectra (21.1 T) of Adip, Bufl, Dicy, Trig, Rani, Dibu, Scop.

	Adip	Bufl	Dicy	Trig	Rani	Dibu	Scop
Pulse sequence	Echo	Echo	Echo	Echo	Echo	Echo	Echo
Number of scans	2048	2048	55280	2048	20480	2048	14080
Recycle delay (s)	1.5	1.5	1.0	1.5	1.0	1.5	1.0
Dwell (μs)	4.0	4.0	4.0	4.0	6.0	4.0	4.0
Spectral width (kHz)	250	250	250	250	167	250	250
Acquisition length (number of points)	512	512	1024	512	1024	512	1024
CT selective 90° pulse width [π/2] (μs)	2.50	2.50	2.0	2.50	2.50	2.50	2.0
CT selective 180° pulse width [π] (μs)	5.00	5.00	4.0	5.00	5.00	5.00	4.0

Table S5. Acquisition parameters for static ^{35}Cl SSNMR spectra (21.1 T) of Mexi, Brom, Alpr, Isop, Aceb, Aman, Proc.

	Mexi	Brom	Alpr	Isop	Aceb	Aman	Proc
Pulse sequence	Echo	Echo	Echo	Echo	Echo	Echo	Echo
Number of scans	10240	41448	41448	41448	2048	1600	41448
Recycle delay (s)	1.0	1.0	1.0	1.0	1.5	1.5	1.0
Dwell (μs)	6.0	4.0	4.0	4.0	4.0	4.0	4.0
Spectral width (kHz)	167	250	250	250	250	250	250
Acquisition length (number of points)	1024	1024	1024	1024	512	512	1024
CT selective 90° pulse width [π/2] (μs)	2.50	1.5	1.5	1.5	2.50	2.50	1.5
CT selective 180° pulse width [π] (μs)	5.00	3.0	3.0	3.0	5.00	5.00	3.0

Table S6. Acquisition parameters for static ^{35}Cl SSNMR spectra (21.1 T) of Isox, Dopa, Amin, IsoxI, MexiI.

	Isox	Dopa	Amin	IsoxI	MexiI
Pulse sequence	Echo	Echo	Echo	Echo	Echo
Number of scans	1600	41448	11520	58240	6800
Recycle delay (s)	1.0	1.0	1.0	1.0	1.0
Dwell (μs)	4.0	4.0	10.0	4.0	4.0
Spectral width (kHz)	250	250	100	250	250
Acquisition length (number of points)	1024	1024	1024	1024	1024
CT selective 90° pulse width [π/2] (μs)	2.50	1.5	2.0	2.0	2.0
CT selective 180° pulse width [π] (μs)	5.00	3.0	4.0	4.0	4.0

Table S7. Acquisition parameters for MAS ^{35}Cl SSNMR spectra (21.1 T) of Adip, Bufl, Dicy, Trig, Rani, Dibu, Scop.

	Adip	Bufl	Dicy	Trig	Rani	Dibu	Scop
Pulse sequence	Echo	Echo	Echo	Echo	Echo	Echo	Echo
Number of scans	6144	5120	6144	6144	10240	19008	1536
Recycle delay (s)	1.0	1.5	1.0	1.0	1.0	3.0	1.0
Dwell (μs)	4.0	4.0	4.0	4.0	6.0	8.0	4.0
Spectral width (kHz)	250	250	250	250	167	125	250
Acquisition length (number of points)	1024	1024	2048	1024	2048	512	2048
CT selective 90° pulse width [π/2] (μs)	2.1	2.1	2.0	2.1	2.0	2.2	2.0
CT selective 180° pulse width [π] (μs)	4.2	4.2	4.0	4.2	4.0	4.4	4.0
Spinning speed (kHz)	22.31	22.35	22	22.33	22.20	21.00	22

Table S8. Acquisition parameters for MAS ^{35}Cl SSNMR spectra (21.1 T) of Mexi, Brom, Alpr, Isop, Aceb, Aman, Proc.

	Mexi	Brom	Alpr	Isop	Aceb	Aman	Proc
Pulse sequence	Echo	Echo	Echo	Echo	Echo	Echo	Echo
Number of scans	10240	6144	6144	6144	6144	3200	6144
Recycle delay (s)	1.0	1.0	1.0	1.0	2.0	1.0	1.0
Dwell (μs)	6.0	4.0	4.0	4.0	8.0	8.0	4.0
Spectral width (kHz)	167	250	250	250	125	125	250
Acquisition length (number of points)	2048	2048	2048	2048	512	2048	2048
CT selective 90° pulse width [π/2] (μs)	2.0	1.5	1.5	1.5	2.2	2.2	1.5
CT selective 180° pulse width [π] (μs)	4.0	3.0	3.0	3.0	4.4	4.4	3.0
Spinning speed (kHz)	22.46	22	22	22	21.72	20.06	22

Table S9. Acquisition parameters for MAS ^{35}Cl SSNMR spectra (21.1 T) of Isox, Dopa, Amin, IsoxI, MexiI.

	Isox	Dopa	Amin	IsoxI	MexiI
Pulse sequence	Echo	Echo	Echo	Echo	Echo
Number of scans	6144	6144	2560	9216	2560
Recycle delay (s)	1.0	1.0	1.0	1.0	1.0
Dwell (μs)	8.0	4.0	20.0	4.0	20.0
Spectral width (kHz)	125	250	50	250	50
Acquisition length (number of points)	2048	2048	2048	2048	2048
CT selective 90° pulse width [π/2] (μs)	2.2	1.5	2.0	2.0	2.0
CT selective 180° pulse width [π] (μs)	4.4	3.0	4.0	4.0	4.0
Spinning speed (kHz)	21.11	22	22	22	22

Table S10. Acquisition parameters for $^{1}H \rightarrow {}^{13}C$ VACP NMR spectra (9.4 T) of Mexi, MexiI, MexiII, Isox, IsoxI.

	Mexi	MexiI	MexiII	Isox	IsoxI
^{1}H $\pi/2$ pulse widths (μs)	2.4	2.4	2.4	2.4	2.4
Hartmann-Hahn matching fields (kHz)	54.4	54.4	54.4	57.9	57.9
Number of scans	40000	40000	16000	8500	9245
Recycle delay (s)	1.0	1.0	1.0	2.0	2.0
Dwell (μs)	20	20	20	20	20
Spectral width (kHz)	50	50	50	50	50
Acquisition length (number of points)	1024	1024	1024	1024	1024
Contact time (ms)	1.5	1.0	5.0	4.0	4.0
^{1}H decoupling fields (kHz)	62.5	62.5	62.5	62.5	62.5
Spinning speed (Hz)	9500	9500	9500	13000	13000

Table S11. Short Cl···H contact distances and angles for HCl pharmaceuticals containing two close Cl···H contacts

Compound	Contact Type	Cl···H Contacts (Å) [a]	C_Q (MHz) [b]	H – Cl – H bond angle (°) [c]	Δ (Å) [d]
Brom	R_3NH^+···Cl	2.020	5.80(3)	117	0.258
	RNH_2···Cl	2.278			
Scop	ROH···Cl	2.101	3.82(3)	115	0.010
	R_3NH^+···Cl	2.111			
Rani	R_3NH^+···Cl	2.017	4.70(10)	101	0.191
	R_2NH···Cl	2.208			
Lido[1]	R_3NH^+···Cl	1.995	4.67(7)	108	0.251
	HOH···Cl	2.246			
Dibu site 1 [e]	R_3NH^+···Cl	2.010	4.65(20)	102	0.351
	R_2NH···Cl	2.361			
Mexi site 1	RNH_3^+···Cl	2.013	5.45(10)	98	0.090
	RNH_3^+···Cl	2.103			

[a] Shortest (< 2.6 Å) Cl···H contacts as determined via first principles energy minimization and geometry optimization. See the experimental section for details. [b] $C_Q = eQV_{33}/h$. [c] Refers to the H – Cl – H bond angle for the two closest hydrogen contacts. [d] Refers to the difference in the two closest H···Cl bond distances. [e] Unable to perform a full or proton geometry optimization due to the large unit cell size and limited computational resources.

Table S12. Short Cl···H contact distances and angles for HCl pharmaceuticals containing three close Cl···H contacts.

Compound	Contact Type	Cl···H Contacts (Å) [a]	Exp. C_Q (MHz) [b]	∠H – Cl – H (°) [c]	Δ (Å) [d]
Alpr	$R_2NH_2^+$···Cl	2.036	5.25(2)	149.70	0.123
	$R_2NH_2^+$···Cl	2.159		73.34	
	ROH···Cl	2.250		89.72	
Isop	ROH···Cl	2.044	5.30(5)	137.05	0.061
	ROH···Cl	2.105		90.29	
	$R_2NH_2^+$···Cl	2.105		118.04	
Proc	R_3NH^+···Cl	2.008	4.25(5)	111.20	0.286
	R_2NH···Cl	2.294		125.41	
	RNH_2···Cl	2.356		119.74	
Aman	RNH_3^+···Cl	2.117	2.90(4)	81.18	0.005
	RNH_3^+···Cl	2.122		79.76	
	RNH_3^+···Cl	2.182		115.92	
Lcme[2]	RNH_3^+···Cl	2.101	2.37(1)	82.20	0.009
	RNH_3^+···Cl	2.110		89.47	
	RNH_3^+···Cl	2.239		108.93	
Aceb	ROH···Cl	2.103	4.57(5)	124.71	0.007
	$R_2NH_2^+$···Cl	2.110		89.05	
	$R_2NH_2^+$···Cl	2.267		100.34	
Lhis[3]	RNH_3^+···Cl	2.168	4.59(3)	77.08	0.044
	RNH_3^+···Cl	2.212		81.50	
	HOH···Cl	2.227		109.34	
Dibu site 2[e]	R_3NH^+···Cl	1.928	4.00(20)	103.40	0.183
	ROH···Cl	2.111		112.56	
	R_2NH···Cl	2.254		111.43	

[a] Shortest (< 2.6 Å) Cl···H contacts as determined via first principles energy minimization and geometry optimization. See the experimental section for details. [b] $C_Q = eQV_{33}/h$. [c] Refers to the H – Cl – H bond angle of the short H···Cl contacts. [d] Refers to the difference in the two H···Cl hydrogen contact bond distances. [e] Unable to perform a full or proton geometry optimization due to the large unit cell size and limited computational resources.

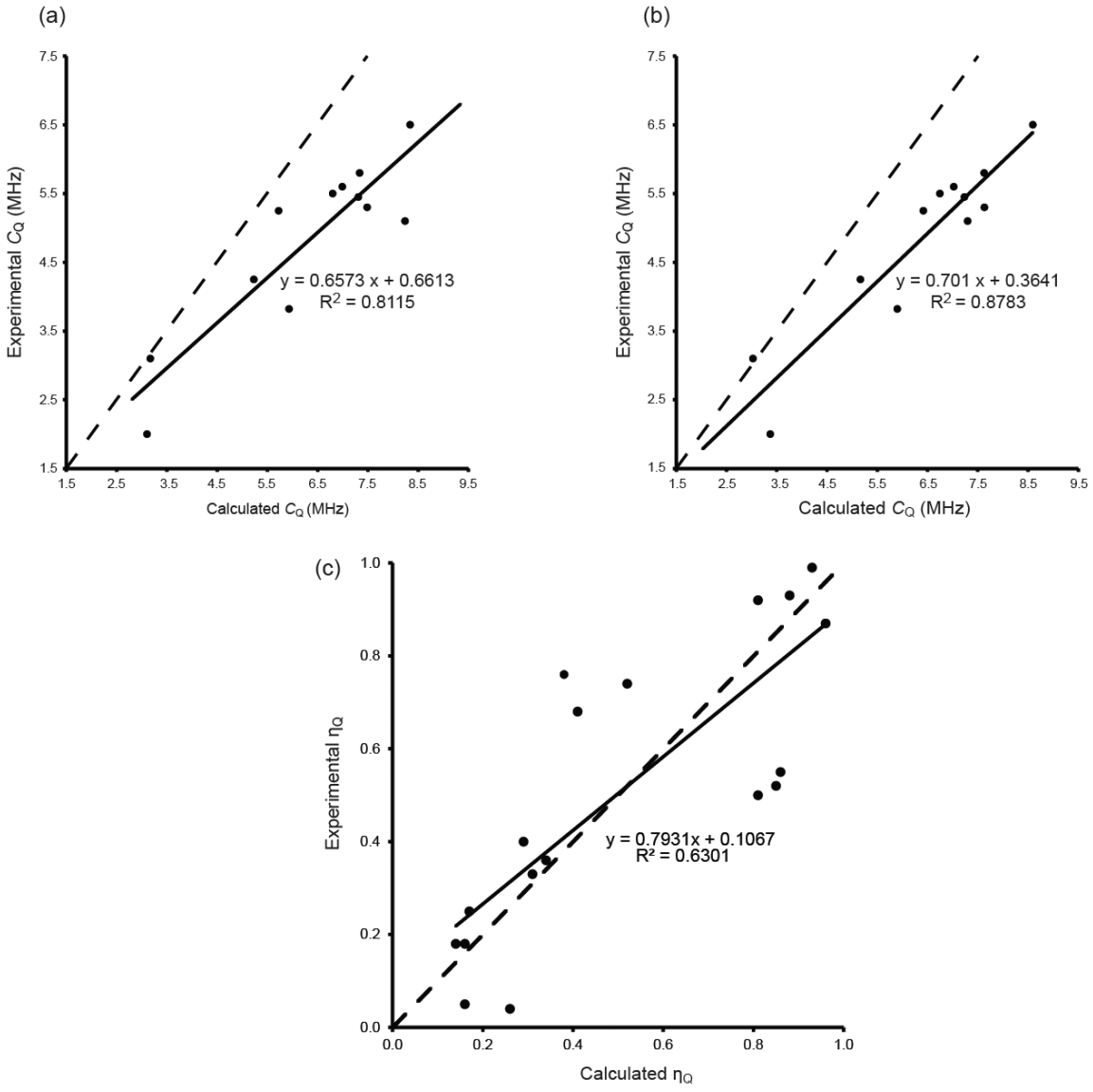

Figure S1. Comparison of the correlation between experimental and calculated values of C_Q on (a) proton optimized structures and (b) fully optimized structures. All calculations were performed using CASTEP.[5-8] The solid line is the line of best fit for the plotted points and the dashed line represents perfect correlation. (c) Correlation between experimental and calculated values of η_Q for fully optimized structures, including those of Amin.

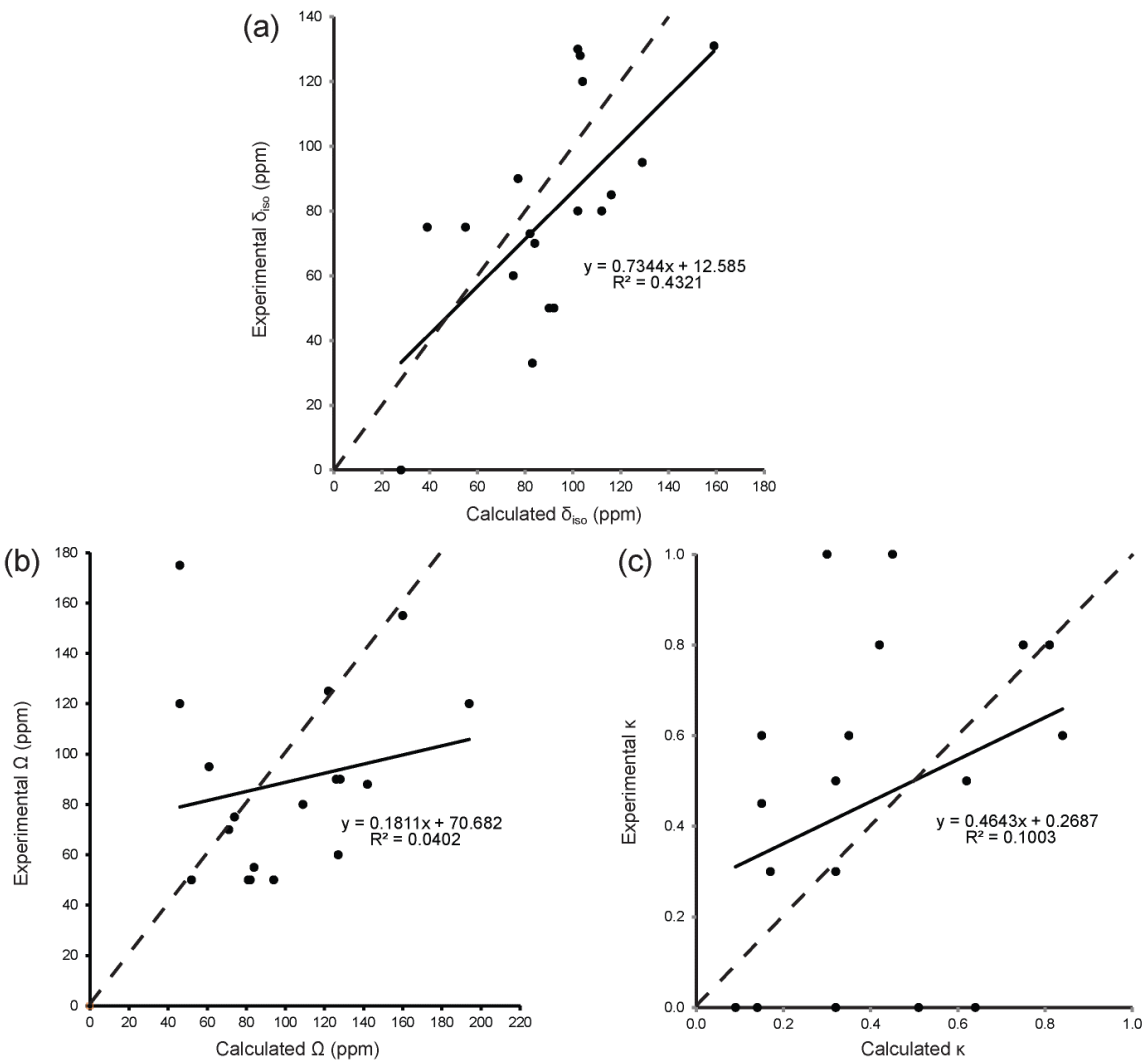

Figure S2. Correlations between experimental and calculated values of (a) δ_{iso}, (b) Ω, and (c) κ. All calculations were performed after full geometry optimization of the structure using CASTEP.[5-8] The solid line is the line of best fit for the plotted points and the dashed line represents perfect correlation.

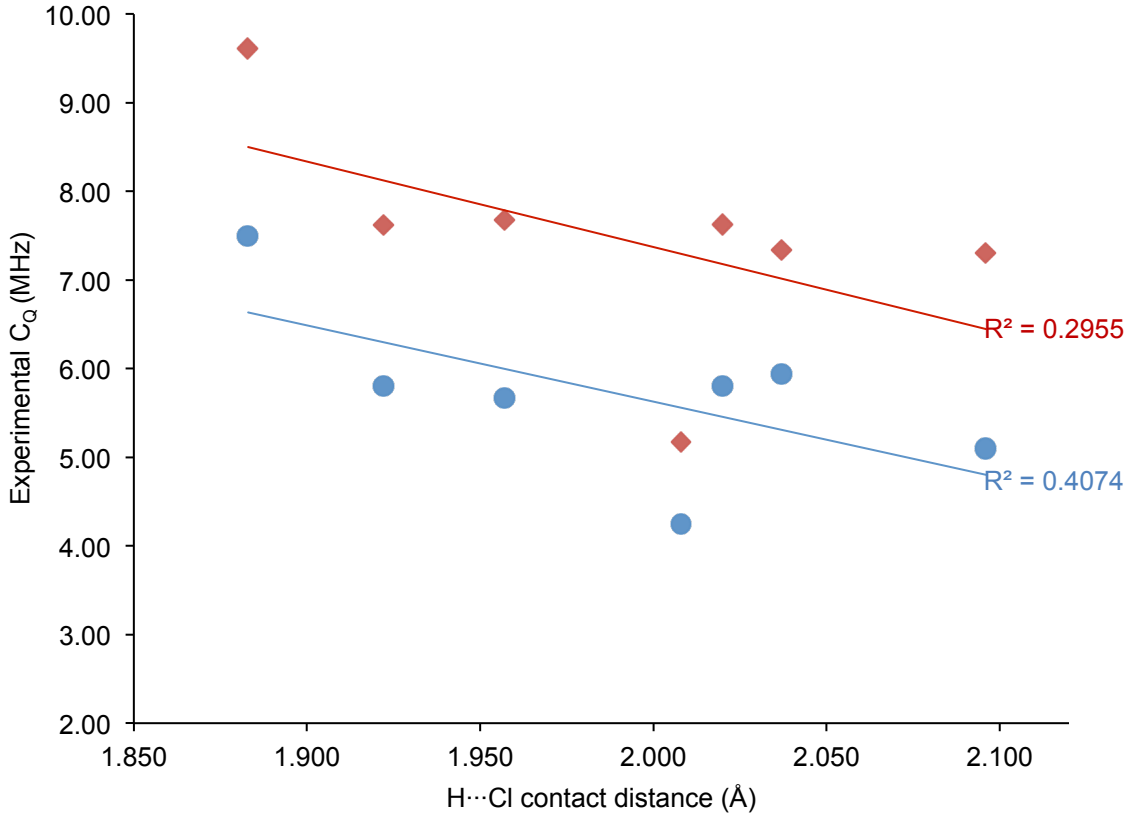

Figure S3. Correlation between experimental (shown in blue) and theoretical (shown in red) values of C_Q and H···Cl bond distances for one-contact API's (Adip, Bufl, Dicy, Trig) and multi-contact API's that involve one contact of ca. 2.0 Å or less (Brom, Proc, Dopa).

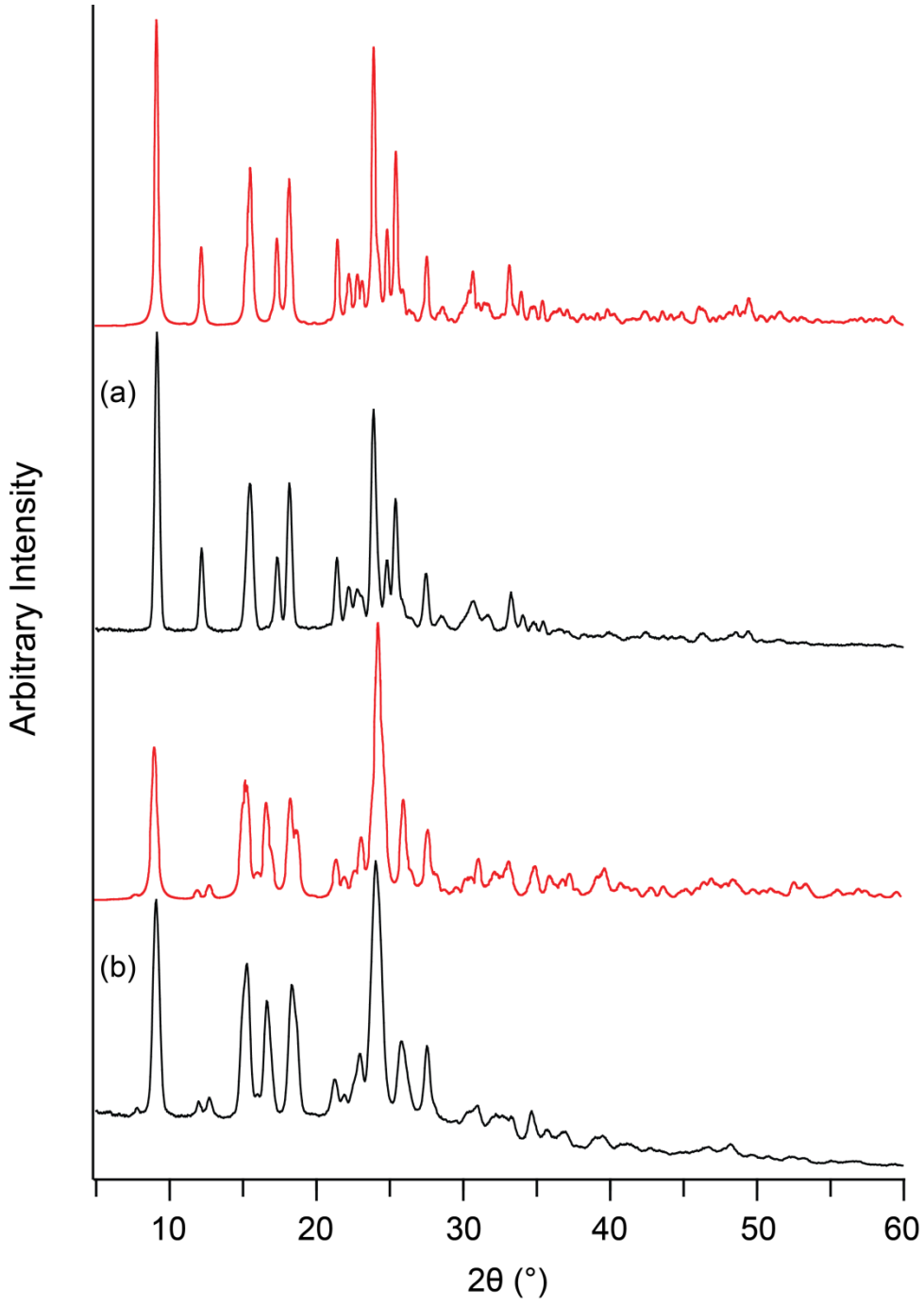

Figure S4. Experimental powder X-ray diffraction patterns of (a) Isox and, (b) IsoxI measured at room temperature. Corresponding simulations are shown in red.

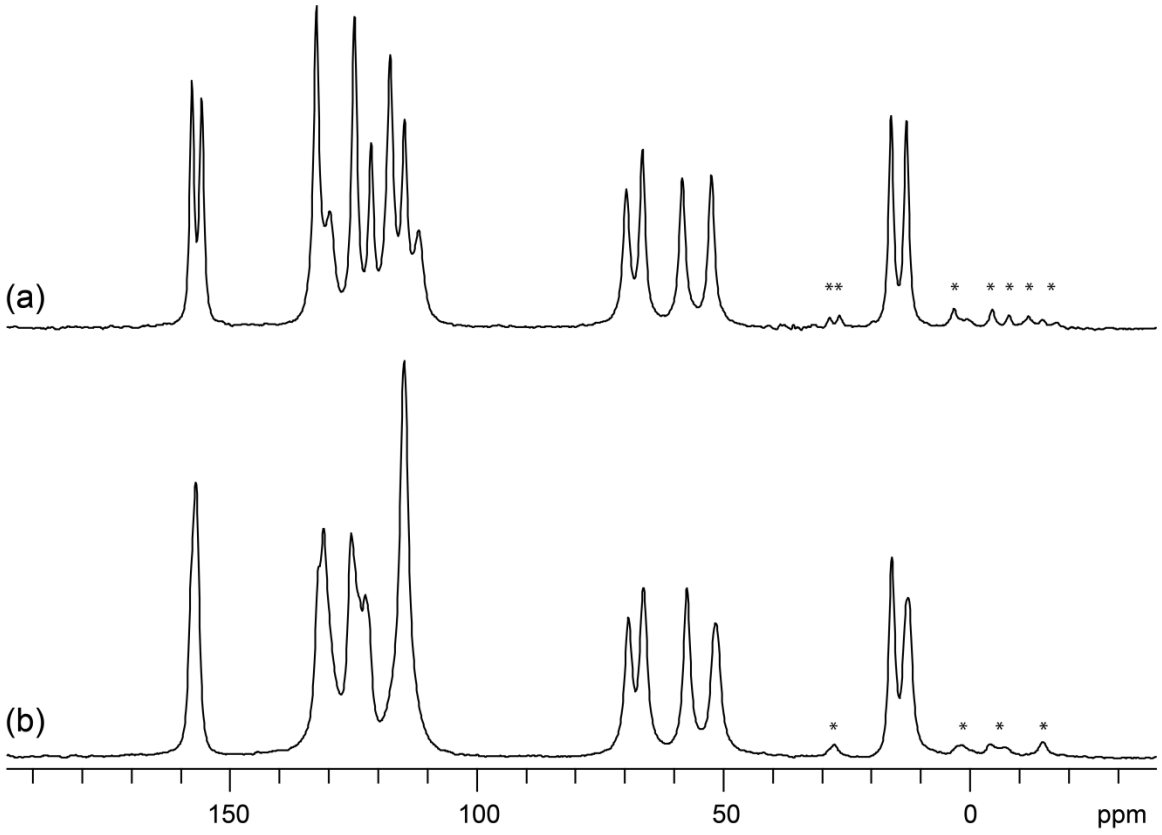

Figure S5. $^{1}H \rightarrow {}^{13}C$ VACP SSNMR spectra (9.4 T) of (a) Isox and, (b) IsoxI. ν_{rot} = 13 kHz. Spinning sidebands denoted by *.

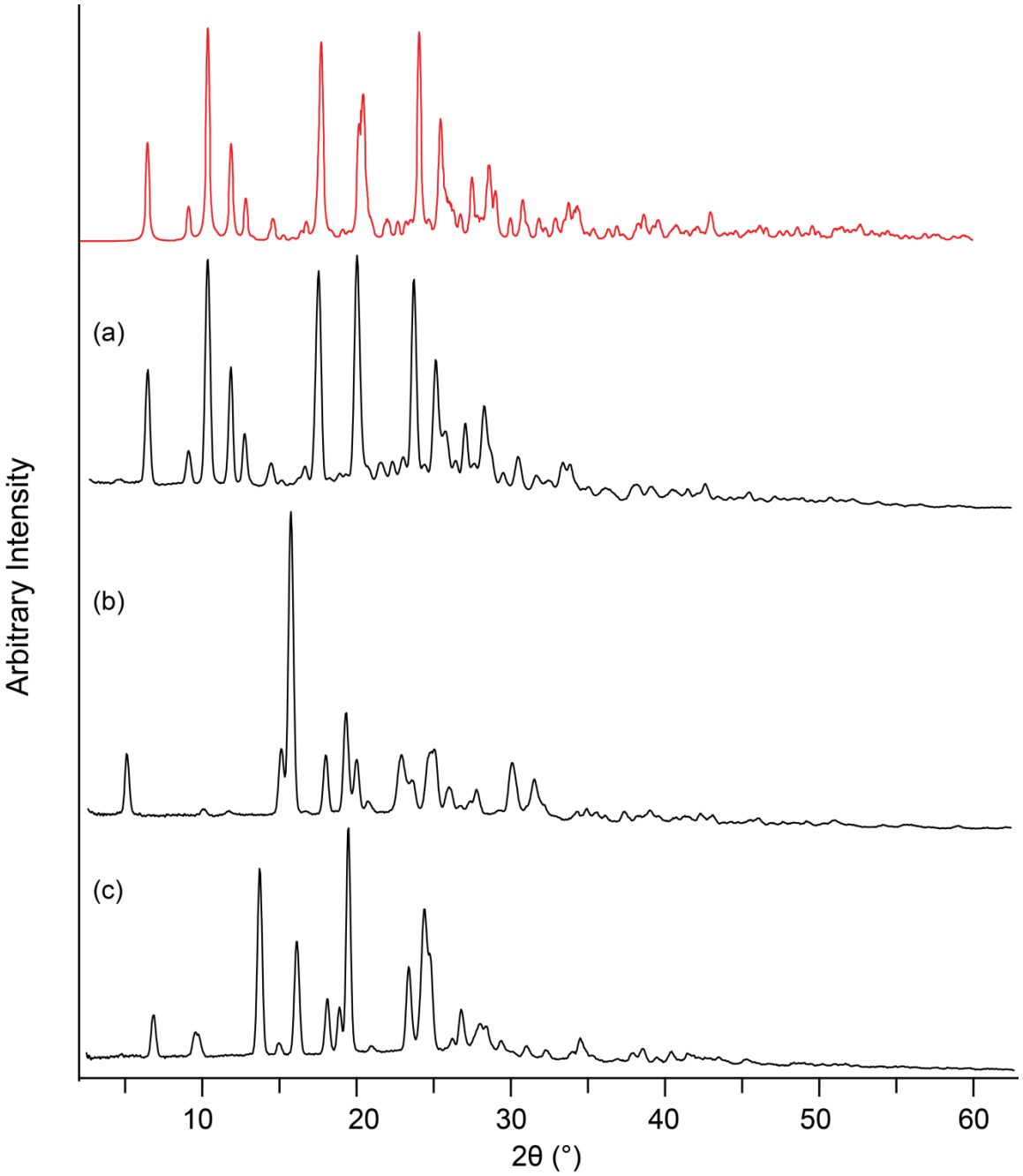

Figure S6. Experimental powder X-ray diffraction patterns of (a) Mexi, (b) MexiI, and (c) MexiII measured at room temperature. The corresponding simulation is shown in red.

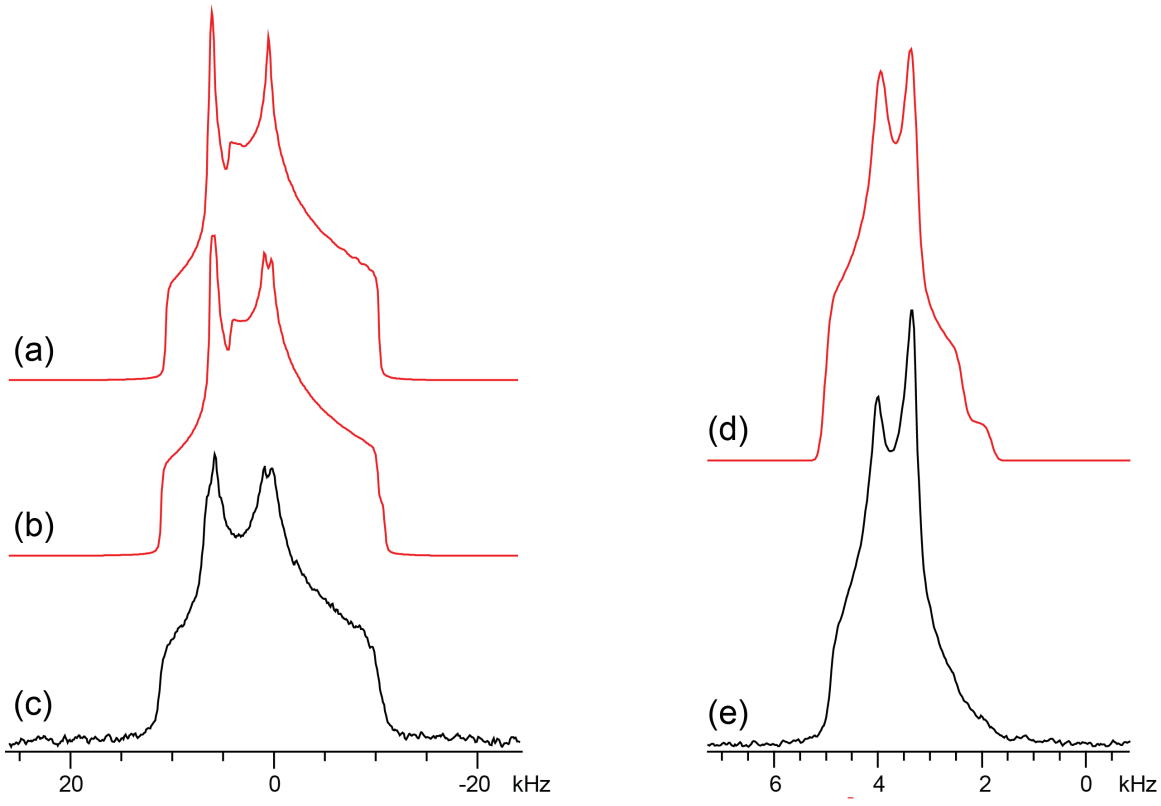

Figure S7. Simulation of the static ^{35}Cl SSNMR spectrum of MexiI (9.4 T) with (a) no CSA contribution and (b) with CSA contribution. Note the splitting of the low frequency horn due to CSA. (c) Experimental static ^{35}Cl SSNMR spectrum of MexiI at 9.4 T. (d) Simulation of the ^{35}Cl MAS SSNMR spectrum of MexiI (21.1 T). (e) Experimental ^{35}Cl MAS SSNMR spectrum of MexiI at 21.1 T.

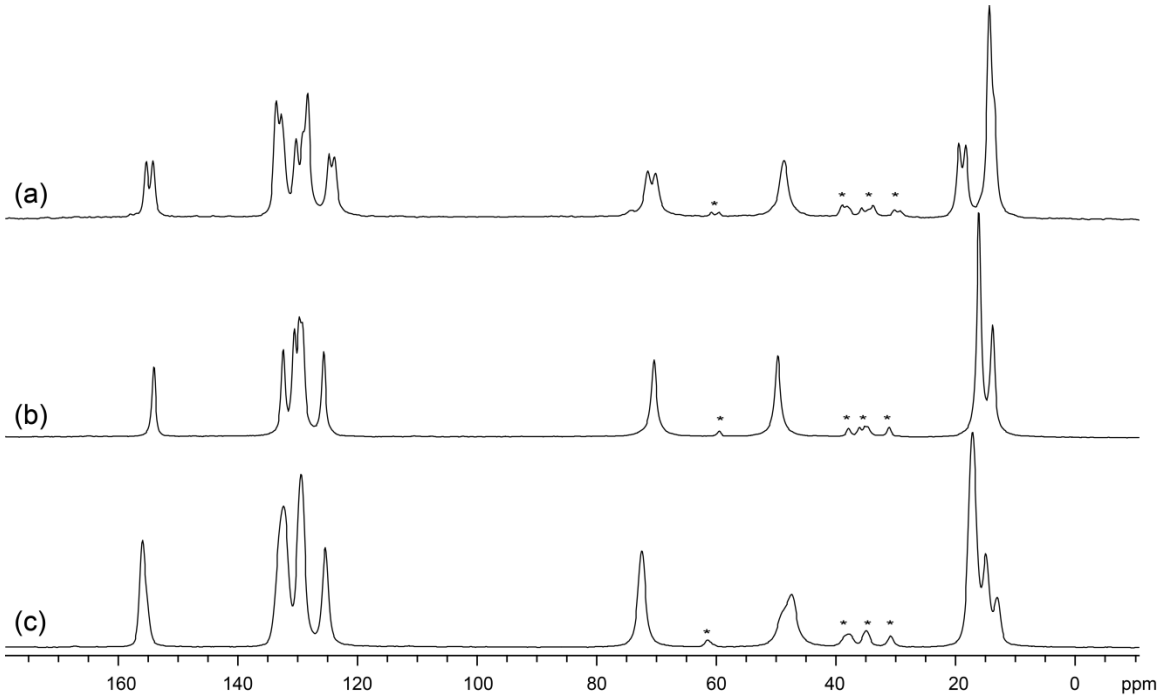

Figure S8. $^{1}H \rightarrow {}^{13}C$ VACP SSNMR spectra (9.4 T) of (a) Mexi, (b) MexiI and, (c) MexiII. ν_{rot} = 9.5 kHz. Spinning sidebands denoted by *.

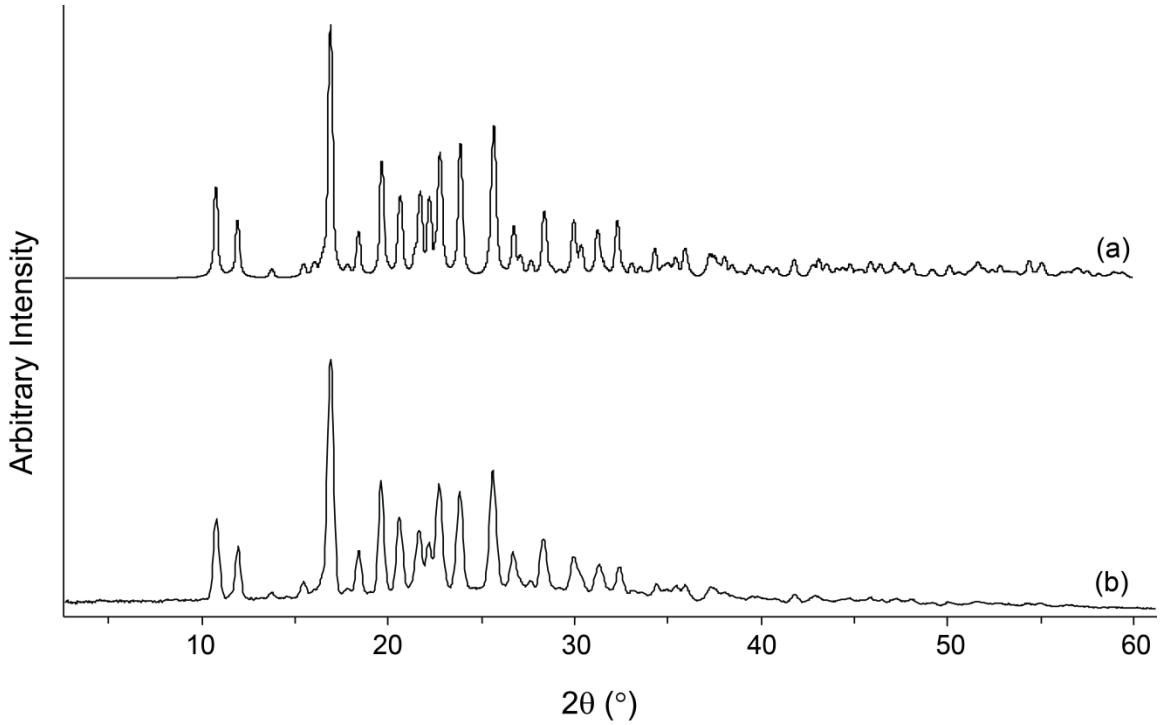

Figure S9. (a) Simulated powder pattern of Proc calculated from previously determined single crystal X-ray diffraction structure[8] and (b) experimental powder X-ray diffraction pattern of Proc measured at room temperature.

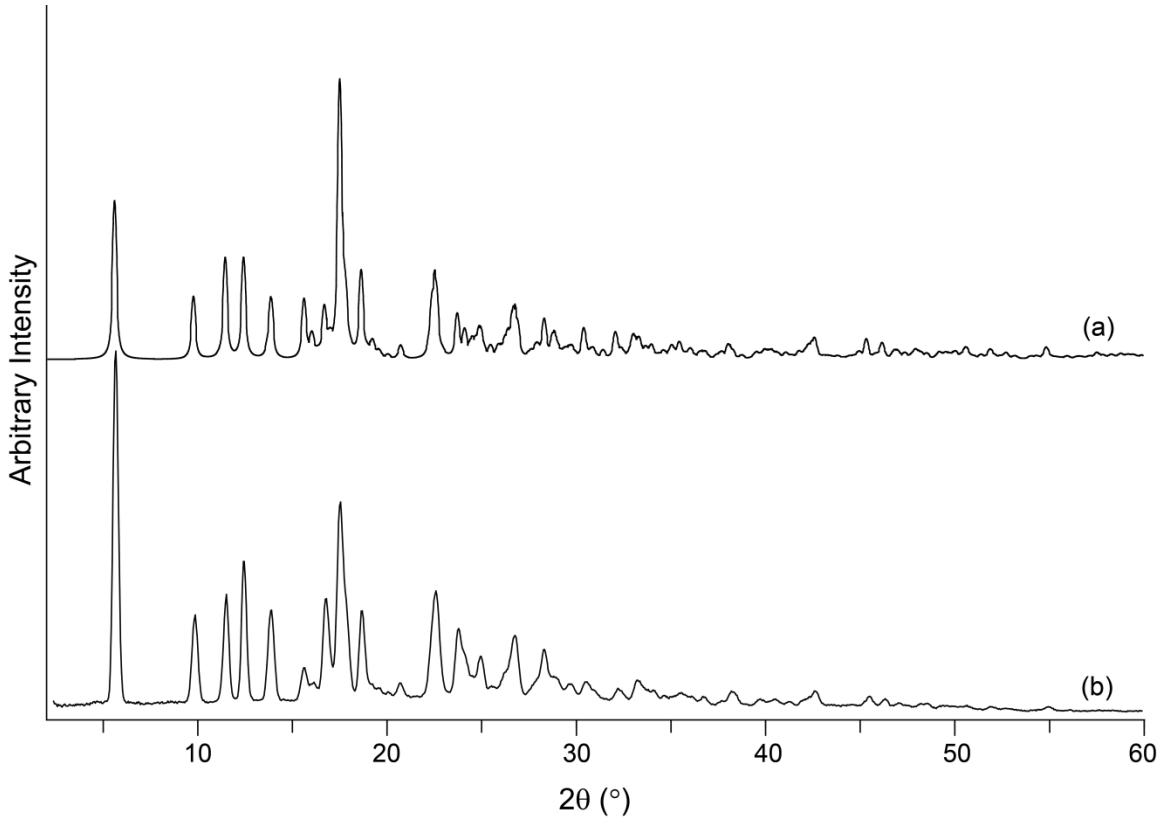

Figure S10. (a) Simulated powder pattern of Dicy calculated from previously determined single crystal X-ray diffraction structure[9] and (b) experimental powder X-ray diffraction pattern of Dicy measured at room temperature.

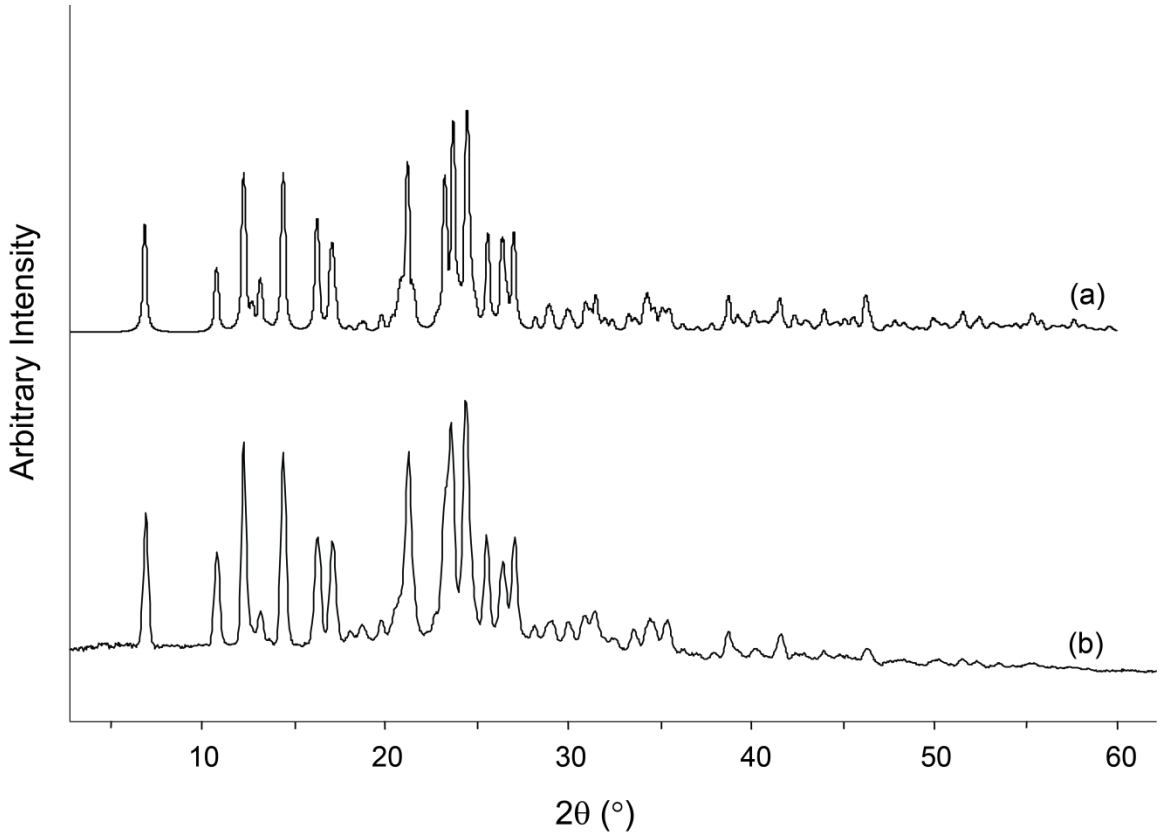

Figure S11. (a) Simulated powder pattern of Alpr calculated from previously determined single crystal X-ray diffraction structure[10] and (b) experimental powder X-ray diffraction pattern of Alpr measured at room temperature.

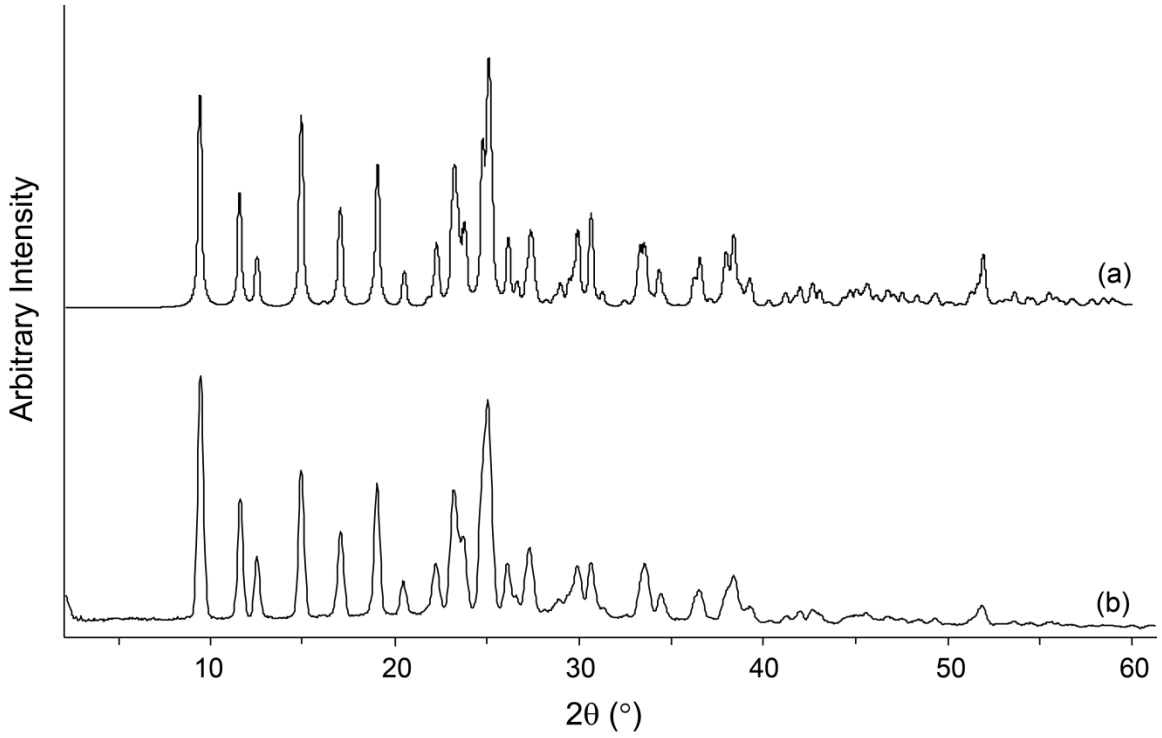

Figure S12. (a) Simulated powder pattern of Isop calculated from previously determined single crystal X-ray diffraction structure[11] and (b) experimental powder X-ray diffraction pattern of Isop measured at room temperature.

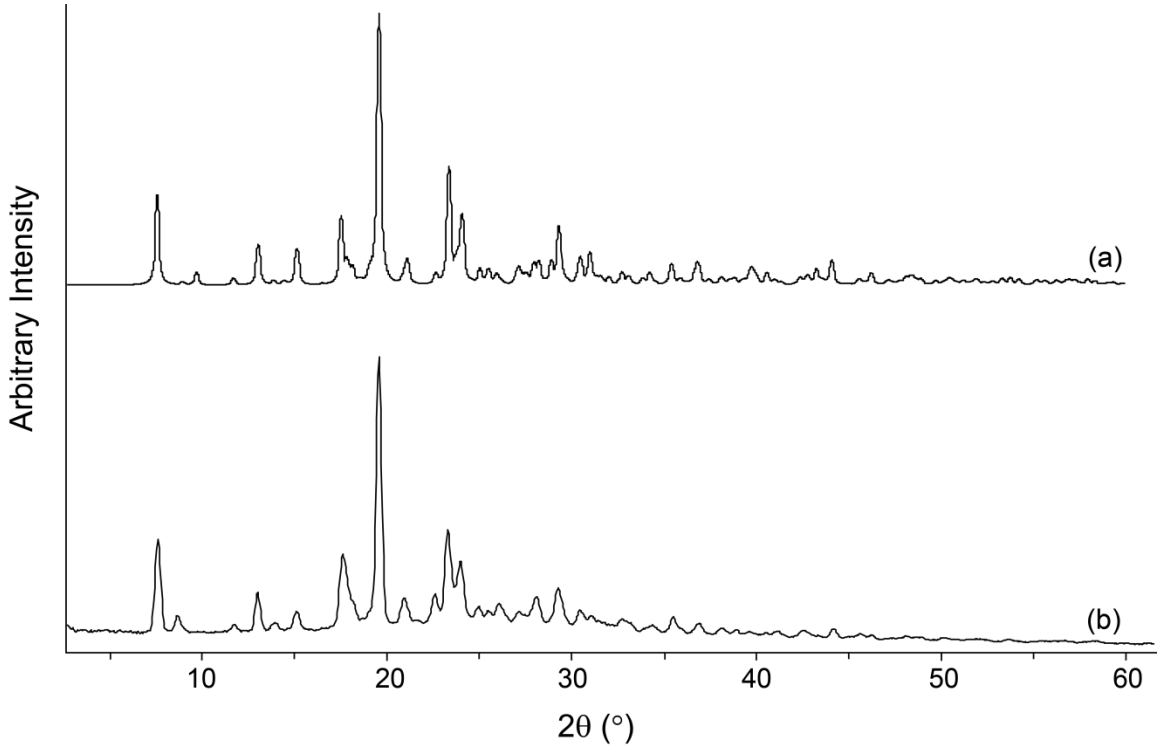

Figure S13. (a) Simulated powder pattern of Nyli calculated from previously determined single crystal X-ray diffraction structure[12] and (b) experimental powder X-ray diffraction pattern of Nyli measured at room temperature.

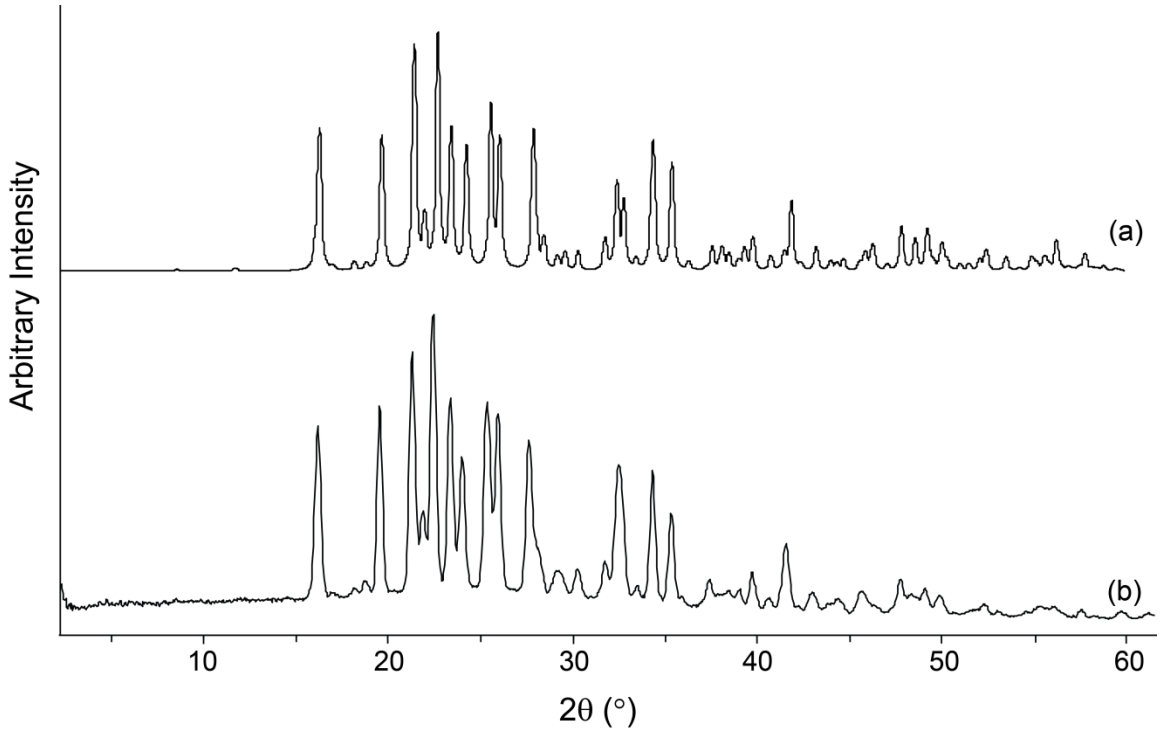

Figure S14. (a) Simulated powder pattern of Dopa calculated from previously determined single crystal X-ray diffraction structure[13] and (b) experimental powder X-ray diffraction pattern of Dopa measured at room temperature.

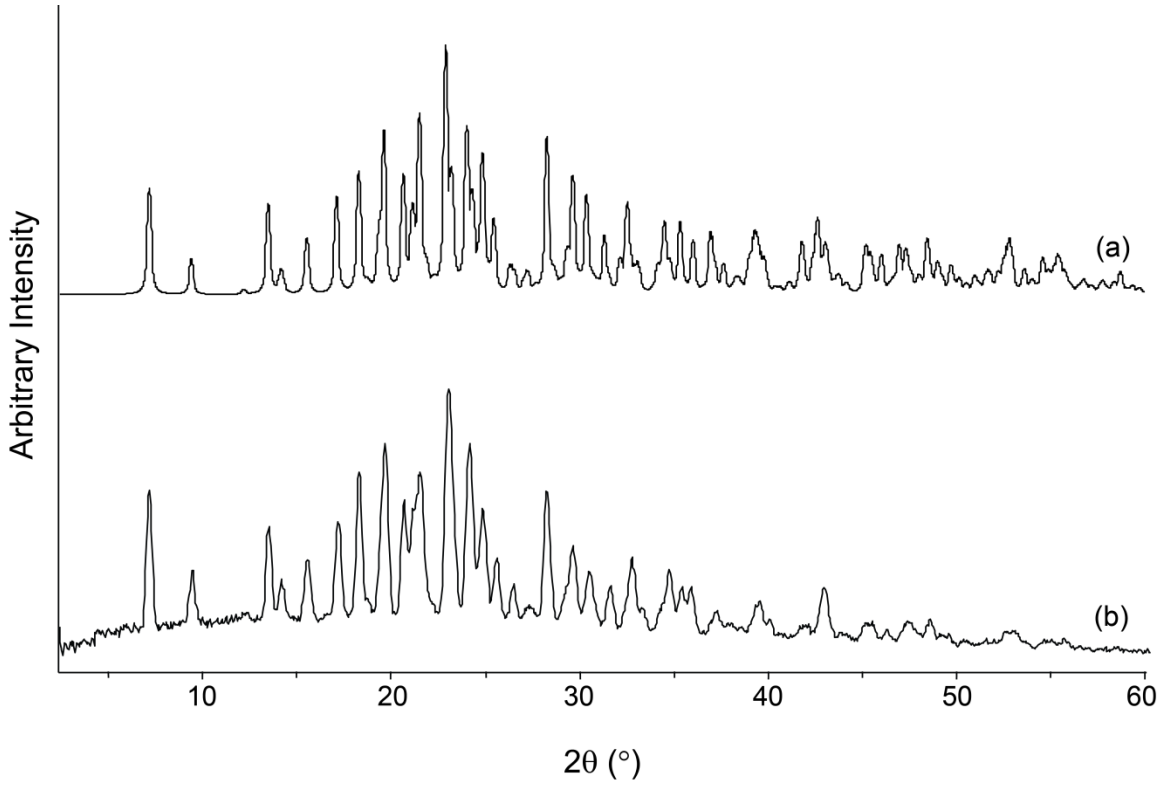

Figure S15. (a) Simulated powder pattern of Brom calculated from previously determined single crystal X-ray diffraction structure[14] and (b) experimental powder X-ray diffraction pattern of Brom measured at room temperature.

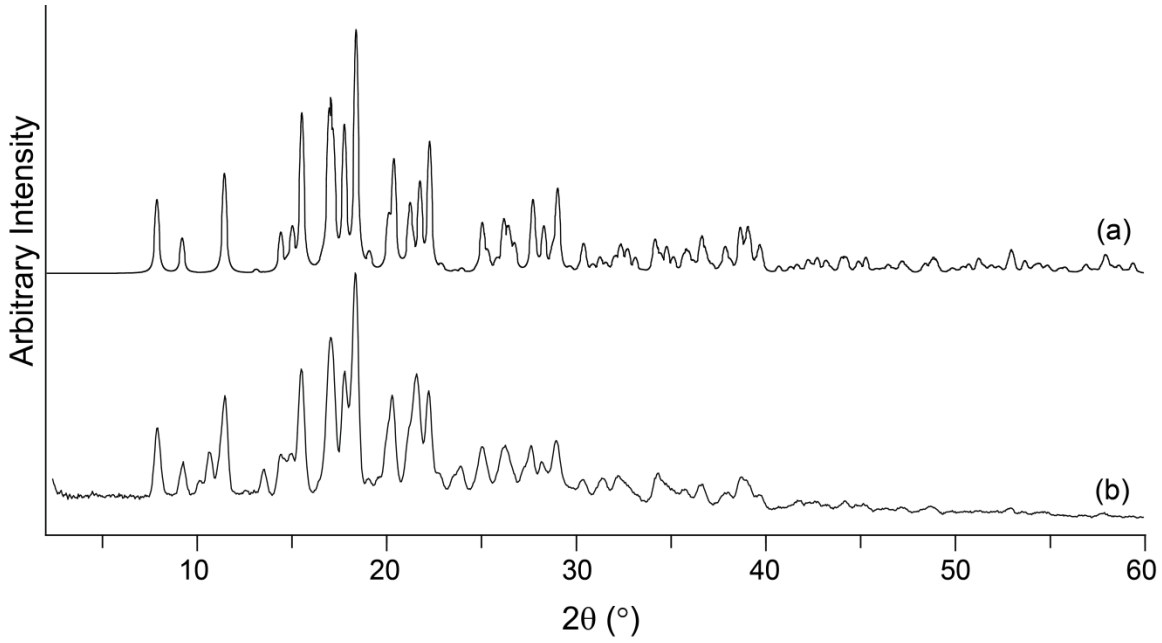

Figure S16. (a) Simulated powder pattern of Scop calculated from previously determined single crystal X-ray diffraction structure[15] and (b) experimental powder X-ray diffraction pattern of Scop measured at room temperature.

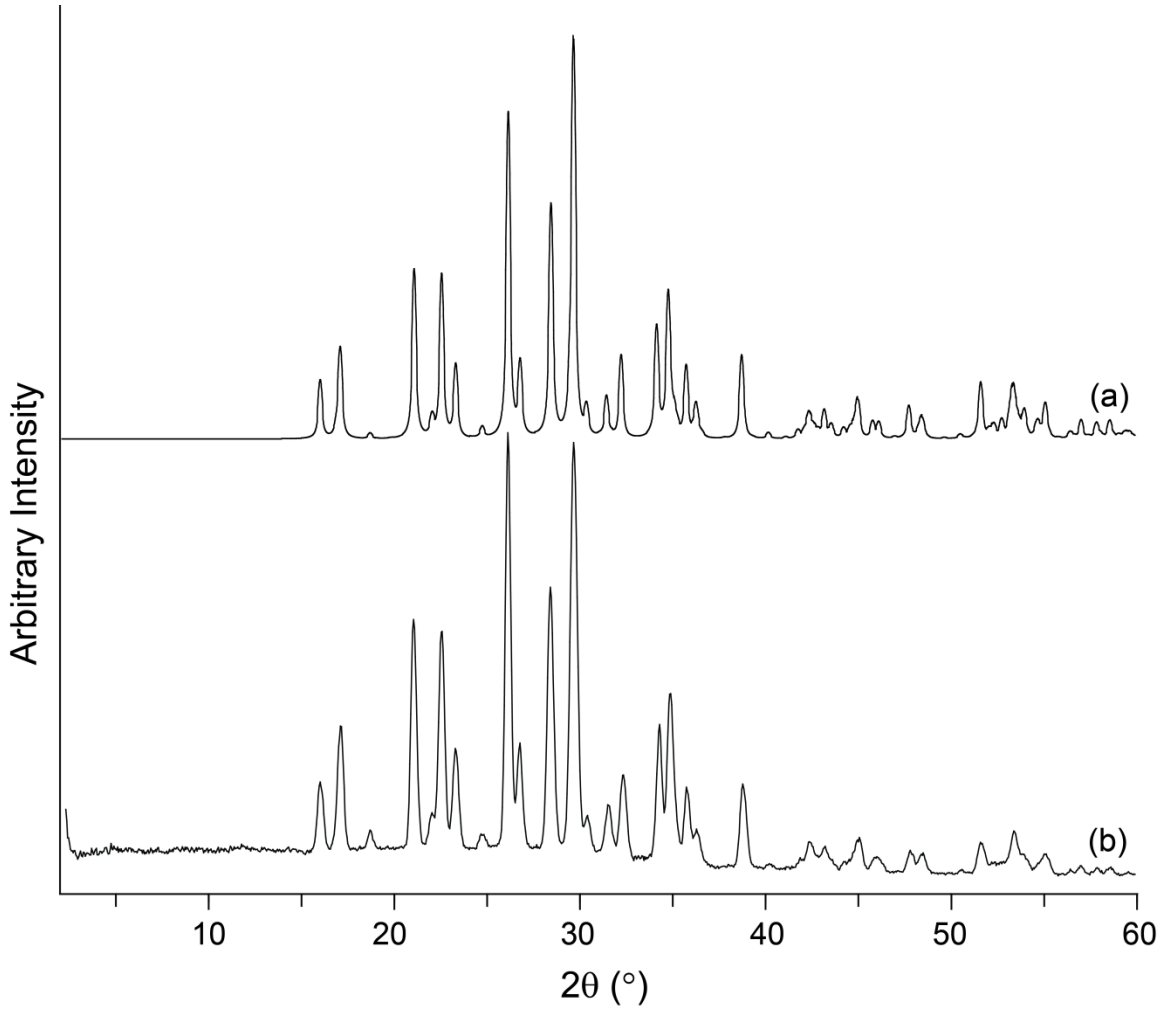

Figure S17. (a) Simulated powder pattern of Amin calculated from previously determined single crystal X-ray diffraction structure[16] and (b) experimental powder X-ray diffraction pattern of Amin measured at room temperature.

References

(1) Hamaed, H.; Pawlowski, J. M.; Cooper, B. F. T.; Fu, R.; Eichhorn, S. H.; Schurko, R. W., *J. Am. Chem. Soc.* **2008**, *130*, 11056-11065.

(2) Bryce, D. L.; Gee, M.; Wasylishen, R. E., *J. Phys. Chem. A* **2001**, *105*, 10413-10421.

(3) Chapman, R. P.; Bryce, D. L., *Phys. Chem. Chem. Phys.* **2007**, *9*, 6219-6230.

(4) Clark, S. J.; Segall, M. D.; Pickard, C. J.; Hasnip, P. J.; Probert, M. J.; Refson, K.; Payne, M. C., *Z. Kristallogr.* **2005**, *220*, 567-570.

(5) Pickard, C. J.; Mauri, F., *Phys. Rev. B.* **2001**, *63*.

(6) Profeta, M.; Mauri, F.; Pickard, C. J., *J. Am. Chem. Soc.* **2003**, *125*, 541-548.

(7) Yates, J. R.; Pickard, C. J.; Mauri, F., *Phys. Rev. B.* **2007**, *76*.

(8) Peeters, O. M.; Blaton, N. M.; Deranter, C. J.; Denisoff, O.; Molle, L., *Cryst.Struct.Commun.* **1980**, *9*, 851-856.

(9) Chananont, P.; Hamor, T. A., *Acta Crystallogr., Sect. B: Struct. Sci.* **1981**, *37*, 1878-1881.

(10) Barrans, Y.; Cotrait, M.; Dangouma.J, *Acta Crystallogr., Sect. B: Struct. Sci.* **1973**, *B 29*, 1264-1272.

(11) Kingsfordadaboh, R.; Hayashi, E.; Haisa, M.; Kashino, S., *Bull. Chem. Soc. Jpn.* **1993**, *66*, 2883-2888.

(12) Leger, J. M.; Goursolle, M.; Carpy, A., *Cryst.Struct.Commun.* **1981**, *10*, 1365-1368.

(13) Giesecke, J., *Acta Crystallogr., Sect. B: Struct. Sci.* **1980**, *36*, 178-181.

(14) Koo, C. H. J., Y. J.; Lee, S. W., *Arch. Pharm. Res.* **1984**, *7*, 115-120.

(15) Glaser, R.; Shiftan, D.; Drouin, M., *Can. J. Chem.* **2000**, *78*, 212-223.

(16) Shvelashvili, A. E.; Tsintsadze, G. V.; Miminoshvili, E. B., *Zh. Neorg. Khim.* **1996**, *41*, 1851-1853.